chemosensors

MDPI

Communication

"Green" Three-Electrode Sensors Fabricated by Injection-Moulding for On-Site Stripping Voltammetric Determination of Trace In(III) and Tl(I)

Maria Pitsou [1], Christos Kokkinos [1], Anastasios Economou [1,*], Peter R. Fielden [2], Sara J. Baldock [2] and Nickolas J. Goddard [3]

[1] Laboratory of Analytical Chemistry, Department of Chemistry, National and Kapodistrian University of Athens, 157 71 Athens, Greece; chemarpi18@gmail.com (M.P.); christok@chem.uoa.gr (C.K.)
[2] Department of Chemistry, Lancaster University, Lancaster LA1 4YB, UK; p.fielden@lancaster.ac.uk (P.R.F.); s.baldock@lancaster.ac.uk (S.J.B.)
[3] Process Instruments (UK) Ltd., March Street, Burnley BB12 0BT, UK; nick.goddard@processinstruments.net
* Correspondence: aeconomo@chem.uoa.gr; Tel.: +30-210-727-4298

Abstract: This work reports the fabrication of a new environmentally friendly three-electrode electrochemical sensor suitable for on-site voltammetric determination of two toxic emerging 'technology-critical elements' (TCEs), namely indium and thallium. The sensor is fully fabricated by injection-moulding and features three conductive polymer electrodes encased in a plastic holder; the reference electrode is further coated with AgCl or AgBr. The sensor is applied to the determination of trace In(III) and Tl(I) by anodic stripping voltammetry using a portable electrochemical set-up featuring a miniature smartphone-based potentiostat and a vibrating device for agitation. For the analysis, the sample containing the target metal ions is spiked with Bi(III) and a bismuth film is electroplated in situ forming an alloy with the accumulated target metals on the working electrode of the sensor; the metals are stripped off by applying a square-wave anodic voltametric scan. Potential interferences in the determination of In(III) and Tl(I) were alleviated by judicious selection of the solution chemistry. Limits of quantification for the target ions were in the low μg L^{-1} range and the sensors were applied to the analysis of lake water samples spiked with In(III) and Tl(I) with recoveries in the range of 95–103%.

Keywords: indium; thallium; anodic stripping voltammetry; injection-moulding; conductive electrodes

Citation: Pitsou, M.; Kokkinos, C.; Economou, A.; Fielden, P.R.; Baldock, S.J.; Goddard, N.J. "Green" Three-Electrode Sensors Fabricated by Injection-Moulding for On-Site Stripping Voltammetric Determination of Trace In(III) and Tl(I). *Chemosensors* **2021**, *9*, 310. https://doi.org/10.3390/chemosensors9110310

Academic Editors: Núria Serrano and Clara Pérez-Ràfols

Received: 7 October 2021
Accepted: 1 November 2021
Published: 3 November 2021

1. Introduction

Indium and thallium belong to the group of "energy-critical elements" or "technology-critical elements" (TCEs); TCEs are elements that had no significant previous industrial role but whose current industrial use is growing rapidly since they are key components in the development of new technologies (information and telecommunications technology, semiconductors, electronic displays, optic/photonic and energy-related technologies) [1–3]. Therefore, TCEs are considered as emerging contaminants and their environmental footprint from anthropogenic and industrial activities should be carefully controlled [4,5]. In particular, the health hazards of both indium [6–8] and thallium [9–11] have been well documented.

Spectroscopic techniques are the "golden standard" for the determination of trace concentrations of indium and thallium [12,13]. However, stripping analysis offers a viable alternative to spectroscopic methods due to its lower cost, rapidity, portability, sensitivity and scope for on-site analysis. The large majority of stripping methods for In and Tl determination are based on the use of mercury-based electrodes that offer excellent sensitivity [2,14]. However, mercury and its vapours are toxic and, over recent years, "green" metals (i.e., bismuth, antimony and tin) have been increasingly used as electrode

materials in stripping analysis [15]. Following this trend, different methods have been developed for the determination of In(III) and Tl(I) on tin [16], bismuth [17,18] and antimony electrodes [19–21].

Injection-moulding is a universal approach for the fabrication of 3D plastic objects in different configurations. Injection-moulding involves feeding the plastic material into a heated barrel, mixing and injecting into a mould cavity, where it cools and hardens to the configuration of the cavity. In the context of electrode fabrication, injection moulding has several advantages over other manufacturing methods: low-cost, scope for mass production, rapidity, wide choice of materials and potential for different geometrical configurations. Our group has reported on the development and application of injection-moulded electrochemical sensors to the determination of Pb(II) and Cd(II) [22–24].

In this work, we describe the development of a new type of integrated injection–moulded sensor which is suitable for field determination of two important and toxic TECs, namely indium and thallium. The device features a plastic holder with three conductive polymer electrodes. The surface of the working electrode is plated in situ with a bismuth film during the analysis. The sensor is adapted to a portable experimental set-up and applied to on-site assay of trace In(III) and Tl(I).

2. Materials and Methods

2.1. Reagents

All the chemicals were of analytical grade and purchased from Merck (Darmstadt, Germany) or Sigma-Aldrich (USA). Doubly distilled water was used throughout. Stock solutions containing 10 and 100 mg L^{-1} of different metals (Bi(III), Cd(II), Sb(III), Pb(II), Sn(II), Zn(II), In(III), Cu(II) and Tl(I)) were prepared from 1000 mg L^{-1} standard solutions after appropriate dilution with doubly distilled water. The stock supporting electrolyte solution was 2.0 mol L^{-1} acetate buffer (pH 4.5) prepared from sodium acetate and hydrochloric acid. Stock aqueous solutions of 2.0 mol L^{-1} KCl, 2.0 mol L^{-1} KBr, 2.0×10^{-3} mol L^{-1} disodium salt of EDTA, and 0.020 mol L^{-1} of $K_4[Fe(CN)_6]$ were also prepared.

2.2. Fabrication of the Sensor

The aluminium moulds were fabricated by creating solid models in AutoCAD (Mechanical Desktop 2004, Autodesk, San Jose, CA, USA) and were converted into macro commands for a CNC milling machine (Datron CAT3D M6, Datron Technology, Milton Keynes, UK). The injection-moulding equipment was Babyplast 6/6 or 6/10 (Cronoplast SL, Barcelona, Spain). The plastic holder was injection-moulded from polystyrene (Northern Industrial Plastics Ltd. Chadderton, UK) (moulding temperature: 220 °C). The polymer electrodes were injection-moulded from 40% carbon fibre-loaded high-impact polystyrene (RTP 487, RTP Company (UK) Plastics Ltd., Bury, UK) (moulding temperature: 220 °C). The three injection-moulded electrodes were inserted into the recesses of the holder using an overmoulding procedure. A photograph of the sensor together its dimensions is shown in Figure 1A; the working area of each of the three electrodes immersed in solution was 40 mm^2.

The reference electrode of the sensor was coated with Ag by spark discharge. To achieve this, an Ag wire was connected as a cathode (−) and the reference electrode of the sensor as an anode (+) to a regulated power supply (0–2.0 KV) and sparking was carried out at 1.2 kV DC by bringing the Ag wire in close proximity to the reference electrode. For Tl(I) and In(III) determination, the reference electrode was coated with a AgCl or a AgBr film, respectively. This was achieved by polarising the Ag-coated reference electrode to +1.0 V for 30 s in a 1.0 mol L^{-1} KCl or 1.0 mol L^{-1} KBr solution using a Pt wire as the counter electrode and a commercial Ag/AgCl as the reference electrode. After use, the sensor was stored with the reference electrode immersed in 0.1 mol L^{-1} KCl or 0.1 mol L^{-1} KBr solution, respectively.

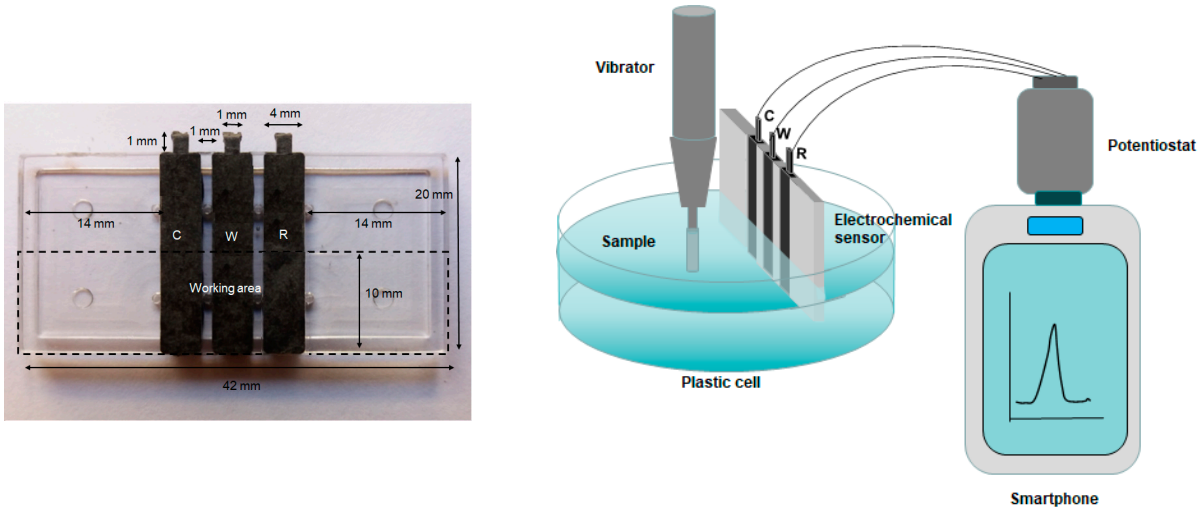

(**A**) (**B**)

Figure 1. (**A**) Photograph of the three-electrode injection-moulded sensor with dimensions, (**B**) schematic diagram of the portable experimental set-up suitable for field measurements.

2.3. Instrumentation and Experimental Set-Up

A schematic diagram of the experimental set up is illustrated in Figure 1B. Electrochemical experiments were performed with a Sensit Smart smartphone-controlled miniature potentiostat via the PSTouch for Android software (Palm Sens BV, The Netherlands). The potentiostat was connected to the injection-moulded sensor with crocodile clips. The sample was placed in a plastic cell and the shaft of a common battery-operated electric toothbrush (Oral B) provided agitation by vibration.

The surface of the working electrode was inspected by means of an optical microscope (Karl Suss PA 200, SUS Microtec).

2.4. Experimental Procedure

The solution was spiked with Bi(III) (and with the appropriate concentration of the target metals as required) and co-deposition of the bismuth film and the analytes at the working electrode was carried out using agitation with vibration. Then, the solution was allowed to equilibrate in static solution for 10 s and the stripping step was performed by the SW mode. Finally, a cleaning step at +0.20 V for 30 s under stirring was applied to clean the electrode by oxidising remains of the bismuth film and target metals on the electrode. The selected experimental conditions for each metal ion are summarised in Table 1.

Table 1. Experimental conditions for Tl(I) and In(III) determination.

	In(III)	**Tl(I)**
Supporting electrolyte	0.10 mol L^{-1} acetate buffer (pH 4.5) + 2.0 × 10^{-5} mol L^{-1} $K_4(Fe(CN)_6]$ + 0.80 mol L^{-1} KBr	0.10 mol L^{-1} acetate buffer (pH 4.5) + 2.0 × 10^{-5} mol L^{-1} EDTA
Deposition potential (V)	−1.40	
Bi(III) concentration (mg L^{-1})	0.50	10
Deposition time (s)	240	
SW frequency (Hz)	25	
SW pulse height (mV)	25	
SW step (mV)	4	
Cleaning time (s)	30	
Cleaning potential (V)	+0.20	

3. Results

The deposition of a bismuth film on the conductive polymer working electrode was examined by optical microscopy. Coating of the electrode's surface with a bismuth film was performed using the set-up of Figure 1B placing a 100 mg L^{-1} Bi(III) solution in 0.1 mol L^{-1} acetate buffer (pH 4.5) in the sample compartment and depositing bismuth on the working electrode at −1.40 V for 120 s. Figure 2A illustrates the surface of the working electrode which is coated with bismuth (left) and the bare electrode surface (right). The presence of a bismuth film on the electrode surface is clearly visible (appearing as the grey deposit in Figure 2A (left)). The presence of the bismuth film is also corroborated by an anodic scan of the bismuth-coated working electrode in which a well-defined oxidation peak of Bi is obtained (Figure 2B).

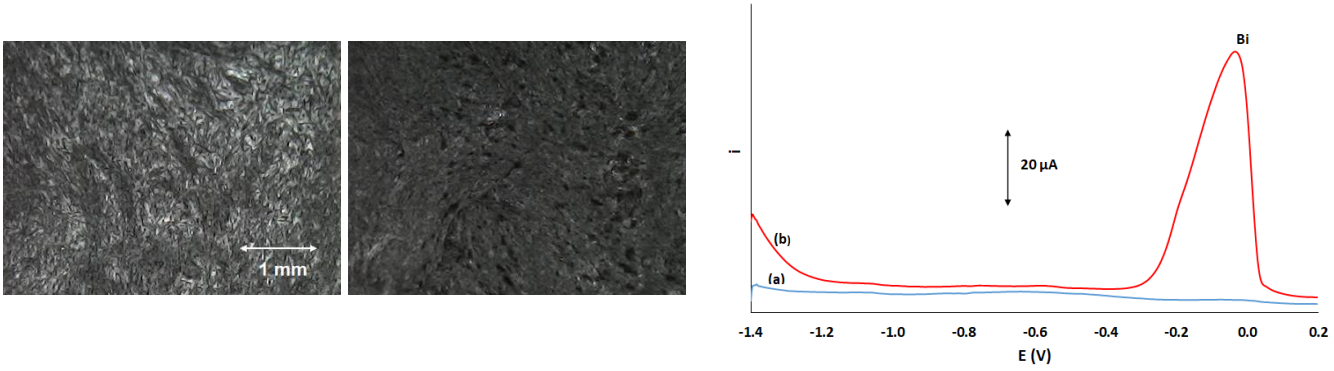

(**A**) (**B**)

Figure 2. (**A**) Optical microscopy image of the working electrode of an injection-moulded sensor showing the bare surface (**right**) and the bismuth-coated surface (**left**), (**B**) stripping voltammogram in: (a) 0.10 mol L^{-1} acetate buffer (pH 4.5), (b) 0.10 mol L^{-1} acetate buffer and 10 mg L^{-1} Bi(III) with deposition at −1.40 V for 20 s.

The main complication in the determination of In(III) and Tl(I) is the interference by co-existing metal ions which can give rise to overlapping stripping peaks [25,26]. Therefore, our first objective was to investigate the effect of cations that are known to oxidise at similar potential to In and Tl or that can exist at relatively higher concentrations (namely Sn(II), Sb(III), Pb(II), Cd(II), Zn(II) and Cu(II)). Initial experiments were carried out in the presence of 0.10 mol L^{-1} acetate buffer (pH 4.5) which is the commonest supporting electrolyte. Figure 3a shows stripping voltammograms of a 10 mg L^{-1} Bi(III) solution in 0.10 mol L^{-1} acetate buffer (pH 4.5) in which only the Bi stripping peak appears. Stripping voltammograms of Tl(I) and In(III) added separately in 10 mg L^{-1} Bi(III) solution in 0.10 mol L^{-1} acetate buffer (pH 4.5) show single stripping peaks of Tl and ln, respectively, together with the Bi peak (Figure 3b,c). Simultaneous addition of Pb(II), Cd(II), Zn(II) and In(III) in 10 mg L^{-1} Bi(III) solution in 0.10 mol L^{-1} acetate buffer (pH 4.5) shows that there is serious overlap between the In peak and the Cd peak (Figure 3d) while further addition of T(l) in the same solution shows serious overlap of the In and Tl peaks and partial overlap between the Pb and Tl peaks (Figure 3e). Addition of Sn(II) and Sb(III) in the same solution did not cause any change of the signal (Figure 3f). Finally, addition of Cu(II) in the same solution caused serious suppression of the total signal (Figure 3g).

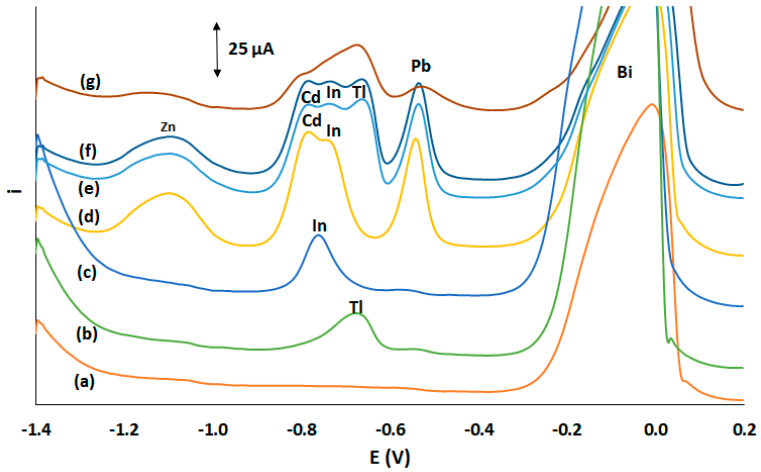

Figure 3. Stripping voltammograms in 0.10 mol L^{-1} acetate buffer (pH 4.5) containing: (a) 10 mg L^{-1} Bi(III) (b) as (a) with 20 µg L^{-1} Tl(II), (c) as (a) with 20 µg L^{-1} In(III), (d) as (c) with 50 µg L^{-1} of Pb(II), Cd(II) and Zn(II), (e) as (d) with 20 µg L^{-1} Tl(I), (f) as (e) with 20 µg L^{-1} Sn(II) and Sb(III), (g) as (f) with 20 µg L^{-1} Cu(II). Deposition at −1.40 V for 240 s.

The interference by Cu(II) on In(III) determination can be alleviated by the addition of $K_4[(Fe(CN)_6]$ which has been shown to selectively complex Cu(II) [27]; as illustrated in Figure 4A(a), a well-defined In peak was obtained in the presence of Cu(II). However, the presence of $K_4[(Fe(CN)_6]$ does not suppress the Cd and Pb peaks that overlap with the In peak (Figure 4A(b). As shown before, addition of Br^- can induce separation of the In and Cd peaks by shifting the Cd peak to more negative values [25]. Different concentrations of KBr were studied in the range 0.1 to 1.0 mol L^{-1}; KBr concentrations ≥0.8 mol L^{-1} were shown to produce the best separation between the Cd and In peaks (Figure 4A(c)). In addition, the concentration of the Bi(III) solution can also affect the separation between the Cd and In peaks [25]. For the determination of In(III), the Bi(III) concentration was studied in the range 0.1 to 20 mg L^{-1} and 0.5 mg L^{-1} was selected as the Bi(III) concentration that leads to better separation between the Cd and In peaks (Figure 4A(d)) while the In peak height remains statistically unaffected.

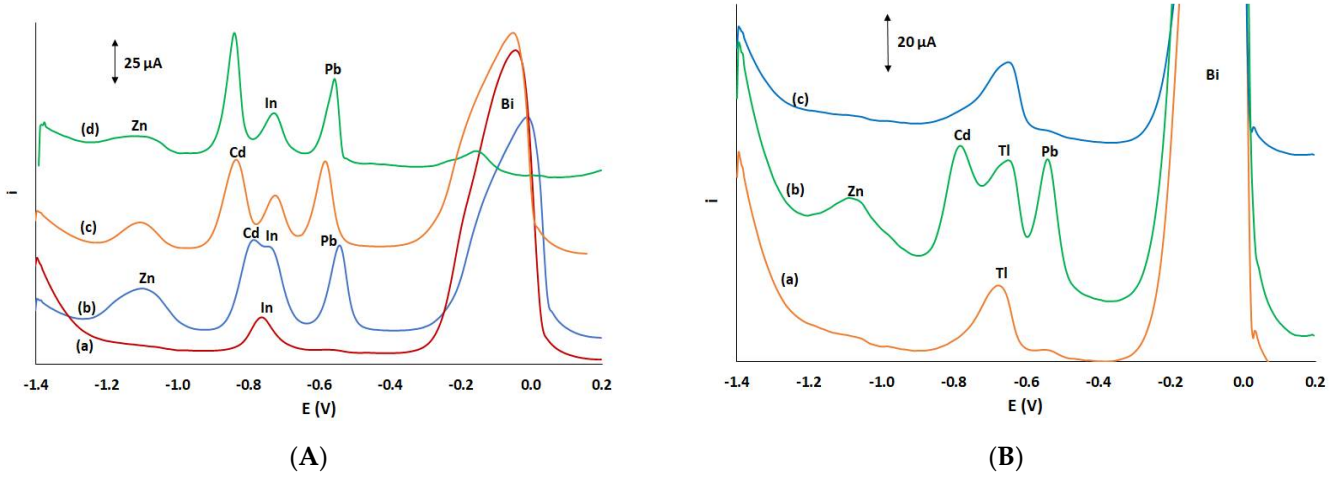

Figure 4. (**A**) Stripping voltammogram in: (a) 0.1 mol L^{-1} acetate buffer (pH 4.5) containing 10 mg L^{-1} Bi(III), 20 µg L^{-1} In(III), 50 µg L^{-1} Cu(II) and 2.0×10^{-5} mol L^{-1} $K_4(Fe(CN)_6]$, (b) as in (a) with 50 µg L^{-1} Pb(II), Cd(II) and Zn(II), (c) as in (b) with addition of 0.8 mol L^{-1} KBr, (d) 0.1 mol L^{-1} acetate buffer (pH 4.5) containing 0.5 mg L^{-1} Bi(III), 20 µg L^{-1} In(III) and 20 µg L^{-1} Cu(II), Pb(II), Cd(II) and Zn(II), (**B**) stripping voltammogram in: (a) 0.1 mol L^{-1} acetate buffer (pH 4.5) containing 10 mg L^{-1} Bi(III) and 40 µg L^{-1} Tl(I), (b) as in (a) with the addition of 50 µg L^{-1} Cd(II), Pb(II) and Zn(II); (c) as in (b) with the addition of 50 µg L^{-1} In(III), Cu(III) and 2.0×10^{-5} mol L^{-1} EDTA.

On the other hand, addition of EDTA alleviates completely the interference by divalent cations on the determination of Tl(I), due to their strong complexation by EDTA (Figure 4B) [26]; while suppressing the Ca, Pb and Cd peaks. addition of EDTA (Figure 4B(c)) does not cause statistically significant change in the Tl peak heigh (Figure 4B(a)).

As a result of this study, the selected conditions for each target metal are listed in Table 1. It must be noted that In(III) and Tl(I) cannot be determined simultaneously using the proposed procedure since their peaks partially overlap. However, it is very unlikely that the two metals will be found in the same sample

Furthermore, the deposition potential was investigated in the range −0.60 V to −1.40 V. The stripping peak heights of both cations increased as the deposition potential became more negative and levelled off at −1.30 V (Figure S1, Supplementary Material) and −1.40 V was elected as the deposition potential. The deposition time was studied in the range 0–360 s and a rectilinear increase in the stripping peak heights of Tl and In vs. the deposition time was observed; a deposition time of 240 s was selected for the sake of more rapid measurements. (Figure S1, Supplementary Material). The shaft of a battery-operated electric toothbrush was selected for solution agitation during preconcentration. This arrangement allowed operation of the experimental set-up without any auxiliary power source. The positioning of the tip of the shaft was important: the tip was placed facing, and at different distances from, the working electrode. The highest stripping peaks were obtained at a separation of 1.5 cm between the working electrode and the tip of the shaft.

The metrological features (calibration equation, coefficient of determination and limits of quantification) of In(III) and Tl(I) determination in the presence of foreign ions were investigated and summarised in Table 2. Representative voltammograms and calibration plots for In(III) and Tl(I) are illustrated in Figure 5A,B, respectively. The limit of detection (LOD) for each metal was calculated from the equation: LOD = 3.3 × s_b/S (where s_b is the standard deviation of the intercept of the calibration plot and S is the slope of the calibration plot) and the limit of quantification (LOQ) from the equation: LOQ = 3 × LOD. The LODs achieved with the injection-moulded sensors compare favourably with existing electrodes modified with "green metals" (Table S1, Supplementary Material).

Table 2. Calibration features of In(III) and Tl(I).

	In(III)	**Tl(I)**
Linear range (μg L^{-1})	3.6–100	4.4–100
Slope (μA $μg^{-1}$ L)	1.02	0.37
Intercept (μA)	0.86	0.43
Coefficient of determination	0.987	0.998
% RSD_b *	14.3%	12.1%
% RSD_w **	5.3%	5.6%
LOD (μg L^{-1}) ***	1.2	1.5
LOQ (μg L^{-1}) ***	3.6	4.4

* Between-sensor relative standard deviation (n = 6) at 20 μg L^{-1}; ** within-sensor relative standard deviation (n = 6) at 20 μg L^{-1}; *** LOQ, limit of quantification; LOD, limit of detection.

The stability of the reference electrode was also assessed. In the case of Tl(I) determination, the reference electrode was coated with a AgCl layer and stability of the reference electrode potential was provided by the Cl^- ions in the supporting electrolyte (Table 1). In the case of In(III) determination, which involves addition of Br^- ions (Table 1), a Ag/AgCl is not stable and the reference electrode was coated with a AgBr layer; in this case, stability of the reference electrode potential was provided by the Br^- ions in the supporting electrolyte (Table 1). Under these conditions, the potential of both reference electrodes varied within ±5% of their mean value in the course of one week. The long-term stability of the

whole sensors was satisfactory as they could be used for tens of measurements without statistically significant change in their response towards the target metals.

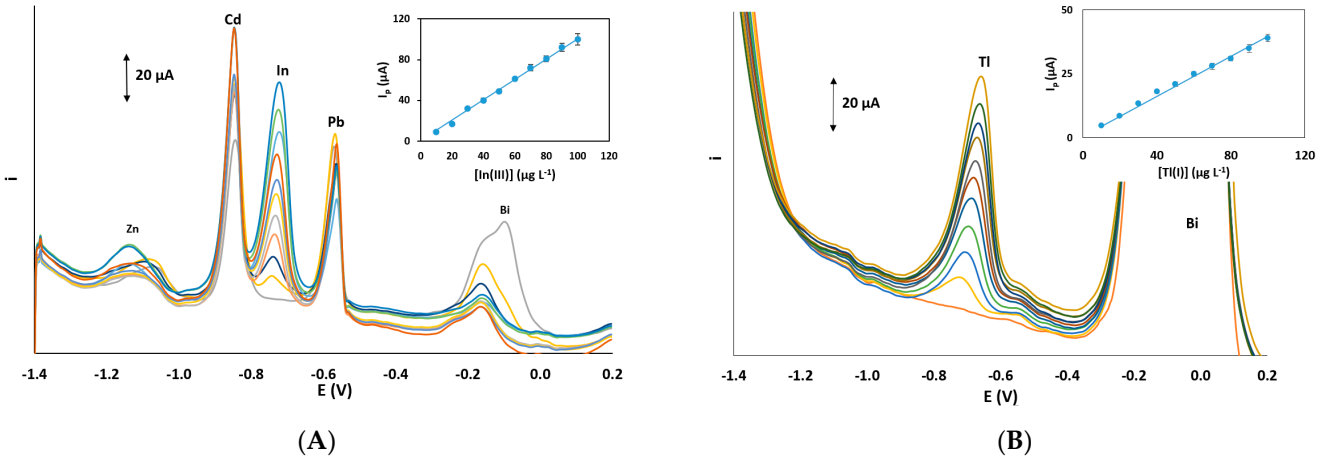

Figure 5. Stripping voltammograms and respective calibration plots (as inserts) for (**A**) In(III), (**B**) Tl(I), in the presence of 100 µg L^{-1} of Cu(II), Zn(II), Pb(II) and Cd(II). Conditions as in Table 1.

The sensors were tested for the determination of In(III) and Tl(I) in a lake water sample. The concentrations of the target metals were lower than the LOQ of the method and the accuracy was assessed by means of spiking the sample with either In(III) or Tl(I) in addition to Cu(II), Zn(II), Pb(II) and Cd(II)) and estimating the recovery using the method of standard additions (Figure 6); the recoveries were 95 ± 6% (n = 3) for In(III) and 103 ± 5% (n = 3) for Tl(I), which are considered satisfactory for rapid on-site testing.

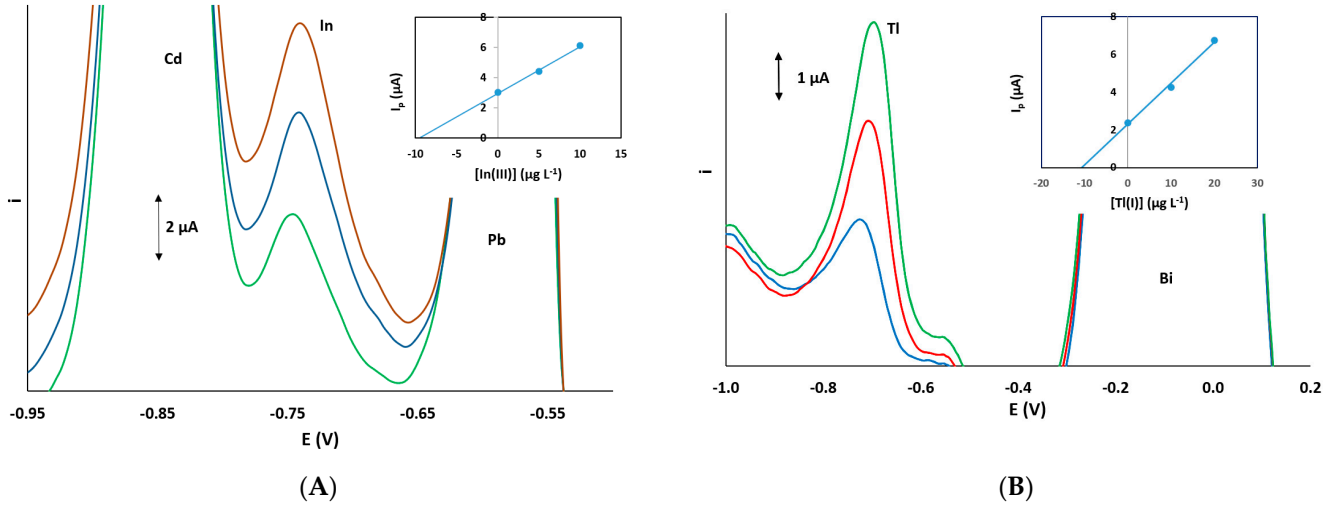

Figure 6. Stripping voltammograms and respective calibration plots (as inserts) for (**A**) In(III), (**B**) Tl(I) determination in a lake water sample spiked with 10 µg L^{-1} of the target metals and 50 µg L^{-1} of Cu(II), Zn(II), Pb(II) and Cd(II). Conditions as in Table 1.

4. Conclusions

In conclusion, this work describes a new type of "green" integrated injection-moulded sensor, which is suitable for on-site analysis of two important TCE elements, In(III) and Tl(I), in conjunction with a portable electrochemical setup. The sensors, when coated in situ with a bismuth film, offer LOQs in the low µg L^{-1} range and adequate selectivity in the presence of common interfering cations.

Supplementary Materials: The following are available online at https://www.mdpi.com/article/10.3390/chemosensors9110310/s1, Figure S1: Effect of (A) the deposition time, (B) the deposition potential in the stripping peak heights of 50 μg L^{-1} In(III) (blue traces) and 50 μg L^{-1} Tl(I) (red traces). Table S1: Comparison of the LODs of the proposed sensors with existing electrodes modified with "green" metals.

Author Contributions: Conceptualisation, A.E., C.K.; methodology, A.E., C.K., P.R.F., S.J.B., N.J.G.; validation, M.P.; writing—original draft preparation, A.E., M.P.; writing—review and editing, A.E., C.K.; supervision, A.E; project administration, A.E.; funding acquisition, A.E. All authors have read and agreed to the published version of the manuscript.

Funding: This research received no external funding.

Institutional Review Board Statement: Not applicable.

Informed Consent Statement: Not applicable.

Data Availability Statement: Data are contained within the article or supplementary material.

Conflicts of Interest: The authors declare no conflict of interest.

References

1. Cobelo-García, A.; Filella, M.; Croot, P.; Frazzoli, C.; Du Laing, G.; Ospina-Alvarez, N.; Rauch, S.; Salaun, P.; Schäfer, J.; Zimmermann, S. COST action TD1407: Network on technology-critical elements (NOTICE)—from environmental processes to human health threats. *Environ. Sci. Pollut. Res.* **2015**, *22*, 15188–15194. [CrossRef]
2. Cobelo-García, A.; Filella, M. Electroanalytical techniques for the quantification of technology-critical elements in environmental samples. *Curr. Opin. Electrochem.* **2017**, *3*, 78–90. [CrossRef]
3. Nuss, P.; Blengini, G.A. Towards better monitoring of technology critical elements in Europe: Coupling of natural and anthropogenic cycles. *Sci. Total Environ.* **2018**, *613–614*, 569–578. [CrossRef]
4. Bu-Olayan, A.H.; Thomas, B.V. Bourgeoning impact of the technology critical elements in the marine environment. *Environ. Pollut.* **2020**, *265*, 115064. [CrossRef]
5. Technology Critical Elements and Their Relevance to the Global Environment Facility. The Scientific and Technical Advisory Panel, UN. 2020. Available online: https://stapgef.org/sites/default/files/2021-02/TCEs%20and%20their%20Relevance%20to%20the%20GEF_web.pdf (accessed on 20 October 2021).
6. White, S.J.O.; Shine, J.P. Exposure Potential and Health Impacts of Indium and Gallium, Metals Critical to Emerging Electronics and Energy Technologies. *Curr. Environ. Health Rep.* **2016**, *3*, 459–467. [CrossRef]
7. Yang, J.L.; Chen, L.H. Toxicity of antimony, gallium, and indium toward a teleost model and a native fish species of semiconductor manufacturing districts of Taiwan. *J. Elem.* **2017**, *23*, 191–199. [CrossRef]
8. Lim, C.H.; Han, J.-H.; Cho, H.-W.; Kang, M. Studies on the Toxicity and Distribution of Indium Compounds According to Particle Size in Sprague-Dawley Rats. *Toxicol. Res.* **2014**, *30*, 55–63. [CrossRef]
9. Toxicological Review of Thallium and Compounds, EPA. 2009. Available online: https://cfpub.epa.gov/ncea/iris/iris_documents/documents/toxreviews/1012tr.pdf (accessed on 20 October 2021).
10. Cvjetko, P.; Cvjetko, I.; Pavlica, M. Thallium Toxicity in Humans. *Arch. Ind. Hyg. Toxicol.* **2010**, *61*, 111–119. [CrossRef]
11. Peter, A.J.; Viraraghavan, T. Thallium: A review of public health and environmental concerns. *Environ. Int.* **2005**, *31*, 493–501. [CrossRef]
12. Jabłońska-Czapla, M.; Grygoyć, K. Speciation and Fractionation of Less-Studied Technology-Critical Elements (Nb, Ta, Ga, In, Ge, Tl, Te): A Review. *Pol. J. Environ. Stud.* **2021**, *30*, 1477–1486. [CrossRef]
13. Filella, M.; Rodushkin, I. A concise guide for the determination of less-studied technology-critical elements (Nb, Ta, Ga, In, Ge, Te) by inductively coupled plasma mass spectrometry in environmental samples. *Spectrochim. Acta Part B At. Spectrosc.* **2018**, *141*, 80–84. [CrossRef]
14. Honeychurch, K.C. Recent Developments in the Stripping Voltammetric Determination of Indium. *World J. Anal. Chem.* **2013**, *1*, 8–13.
15. Ariño, C.; Serrano, N.; Díaz-Cruz, J.M.; Esteban, M. Voltammetric determination of metal ions beyond mercury electrodes. A review. *Anal. Chim. Acta* **2017**, *990*, 11–53. [CrossRef]
16. Kokkinos, C.; Economou, A. Tin film sensor with on-chip three-electrode configuration for voltammetric determination of trace Tl(I) in strong acidic media. *Talanta* **2014**, *125*, 215–220. [CrossRef]
17. Di Martos, L.M.; Jost, C.L. Sequential determination of five heavy metal ions in Brazilian phosphate fertilizers and surface waters by stripping voltammetry. *Int. J. Environ. Sci. Technol.* **2019**, *16*, 6535–6546. [CrossRef]
18. Kozak, J.; Tyszczuk-Rotko, K.; Rotko, M. Voltammetric screen-printed carbon sensor modified with multiwalled carbon nanotubes and bismuth film for trace analysis of thallium(I), *Physicochem. Probl. Miner. Process.* **2019**, *55*, 1422–1428.
19. Zhang, J.; Shan, Y.; Ma, J.; Xie, L.; Du, X. Simultaneous Determination of Indium and Thallium Ions by Anodic Stripping Voltammetry Using Antimony Film Electrode. *Sensor Lett.* **2009**, *7*, 605–608. [CrossRef]

20. Sopha, H.; Baldrianova, L.; Tesarova, E.; Hocevar, S.B.; Svancara, I.; Ogorevc, B.; Vytras, K. Insights into the simultaneous chronopotentiometric stripping measurement of indium(III), thallium(I) and zinc(II) in acidic medium at the in situ prepared antimony film carbon paste electrode. *Electrochim. Acta* **2010**, *55*, 7929–7933. [CrossRef]
21. Bobrowski, A.; Putek, M.; Zarebski, J. Antimony Film Electrode Prepared In Situ in Hydrogen Potassium Tartrate in Anodic Stripping Voltammetric Trace Detection of Cd(II), Pb(II), Zn(II), Tl(I), In(III) and Cu(II). *Electroanalysis* **2012**, *24*, 1071–1078. [CrossRef]
22. Kokkinos, C.; Economou, A.; Goddard, N.J.; Fielden, P.R.; Baldock, S.J. Determination of Pb(II) by sequential injection/stripping analysis at all-plastic electrochemical fluidic cells with integrated composite electrodes. *Talanta* **2016**, *153*, 170–176. [CrossRef]
23. Christidi, S.; Chrysostomou, A.; Economou, A.; Kokkinos, C.; Fielden, P.R.; Baldock, S.J.; Goddard, N.J. Disposable Injection Molded Conductive Electrodes Modified with Antimony Film for the Electrochemical Determination of Trace Pb(II) and Cd(II). *Sensors* **2019**, *19*, 4809. [CrossRef]
24. Partheni, B.; Svarnias, K.; Economou, A.; Kokkinos, C.; Fielden, P.R.; Baldock, S.J.; Goddard, N.J. Voltammetric Determination of Trace Heavy Metals by Sequential-injection Analysis at Plastic Fluidic Chips with Integrated Carbon Fiber-based Electrodes. *Electroanalysis* **2021**, *33*, 1930–1935. [CrossRef]
25. Charalambous, A.; Economou, A. A study on the utility of bismuth-film electrodes for the determination of In(III) in the presence of Pb(II) and Cd(II) by square wave anodic stripping voltammetry. *Anal. Chim. Acta* **2005**, *547*, 53–58. [CrossRef]
26. Kokkinos, C.; Raptis, I.; Economou, A.; Speliotis, T. Determination of Trace Tl(I) by Anodic Stripping Voltammetry on Novel Disposable Microfabricated Bismuth-Film Sensors. *Electroanalysis* **2010**, *22*, 2359–2365. [CrossRef]
27. Kadara, R.O.; Tothill, I.E. Resolving the copper interference effect on the stripping chronopotentiometric response of lead(II) obtained at bismuth film screen-printed electrode. *Talanta* **2005**, *66*, 1089–1093. [CrossRef]